ISSN (Print) 1226-1750
ISSN (Online) 2233-6656
Journal of Magnetics 28(3), 234-238 (2023) https://doi.org/10.4283/JMAG.2023.28.3.234

Polyvinylpyrrolidone-assisted Solvothermal Synthesis of Fe_3O_4 Nanoclusters

Rachida Lamouri and Ki Hyeon Kim*

[1]*Department of Physics, Yeungnam University, Gyeongsan 38541, Republic of Korea*

(Received 3 August 2023, Received in final form 21 September 2023, Accepted 25 September 2023)

We report in this work the effects of the Polyvinylpyrrolidone (PVP) concentration on the solvothermal synthesis of Fe_3O_4 nanocluster with different PVP concentrations such as 5 mg/ml, 10 mg/ml, and 25 mg/ml. The effect of the PVP on the structural, microstructural, and magnetic properties was analyzed using different techniques. XRD patterns showed the crystallization of all samples in the cubic structure with an average crystallite size smaller than 10 nm. Homogeneous dispersion of the nanoparticles was shown for small concentrations of PVP, while the aggregation of the nanoparticles was observed for higher concentrations leading to the formation of uniform nanoclusters with an average size around 167 nm for a PVP concentration of 25 mg/ml. A soft ferromagnetic behavior was found for all prepared samples with a saturation magnetization of about 54.75 emu/g obtained for Fe_3O_4 nanoparticles with 10 mg/ml of PVP.

Keywords : Fe_3O_4 nanocluster, solvothermal synthesis, PVP concentration, magnetic properties

1. Introduction

Iron oxide nanoparticles consist of a combination of iron and oxygen atoms in a specific stoichiometry and structure, where magnetite is known as the most abundant material in the spinel ferrite family, which consists of 8 tetrahedral sites occupied by Fe^{3+} cations, and 16 octahedral sites shared between Fe^{2+} and Fe^{3+} cations, and referred to as a 100 % inverse spinel structure [1-3]. For multiple different reasons, Iron oxide nanoparticles are considered the most suitable and adequate materials for a wide range of industrial and technological applications. However, the aggregation of the iron oxide nanoparticles because of their magnetic interactions limits their applicability in superparamagnetic ferrofluid-based medical applications. To prevent this agglomeration, different strategies were found in the literature where some polymers and organic agents have been used as an interface layer to block the aggregation of the nanoparticles [4-6] in complicated synthesis process to guarantee the reproducibility of the monodispersed nanoparticles.

Thanks to their interesting properties that combine single nanoparticle properties and inter-particle interactions, magnetic nanoclusters have attracted the interest of researchers for biomedical applications [7-9]. By assembling numerous small single nanoparticles, nanoclusters can play an important role in overcoming the limitations due to the superparamagnetic issue in the aggregated nanoparticles by sustaining the superparamagnetic character while increasing the magnetic moments through the interparticles magnetic interactions in addition to the spin magnetic moments of the nanoparticles [10-12].

Enormous efforts have been recently devoted to the synthesis of iron oxide nanoclusters with controlled uniform shape and homogenous size distribution of the nanoclusters. However, the choice of the preparation pathway is closely related to the structure and properties of the nanoparticles where the physicochemical properties of the nanocluster can be completely changed by a small variation in the synthesis process [13-15].

Generally, Iron oxide nanoclusters can be prepared by controlling the aggregation of ultrafine nanoparticles during the synthesis process, or at the end of the synthesis by assembling the ligand-capped fine nanoparticles [13]. Counter to the ligand-capped assembly method which generally requires two steps to produce nanoclusters, the controlled aggregation of the nanoparticles during the synthesis is based on one-step synthesis such as thermal decomposition, solvothermal, and polyol methods in which the nanocluster properties can be adjusted by controlling the synthesis parameters [16-18].

Even though many researchers have been using the

©The Korean Magnetics Society. All rights reserved.
*Corresponding author: Tel: +82-53-810-2334
Fax: +82-53-810-4616, e-mail: kee1@ynu.ac.kr

© 2023 Journal of Magnetics

thermal decomposition method to synthesize controlled shapes and sizes of magnetic iron oxide nanoclusters, the solvothermal method has proven its efficiency and attracted researchers for many reasons, such as the possibility to use different kinds of organic acids as the capping molecules, easily control the size of the nanoclusters by controlling the proportions of the used reactants [19], in addition to the possibility for scale-up production without affecting the properties of the prepared nanoclusters compared to the laboratory scale production [7].

Polyvinylpyrrolidone (PVP) is a commonly stabilizer non-toxic polymer used to prevent the aggregation of the nanoparticles thanks to the existing hydrophobic carbon chains which extend into the solvent through the well-known steric hindrance effect [20, 21].

This work aims to investigate the effect of the PVP concentrations on the dispersion of iron oxide nanoparticles and the formation of nanoclusters using a facile one-pot solvothermal synthesis, which would help control the production of dispersed nanoparticles and nanoclusters.

2. Experiments

The solvothermal route with ethylene glycol as s olvent is used to synthesize Fe_3O_4 nanoparticles where $Fe(NO_3)_3 \cdot 9H_2O$ (Sigma Aldrich, ≥99%) was used as starting precursor. Dissolved Polyvinylpyrrolidone in DI water with three different concentrations (5 mg/ml, 10 mg/ml, and 25 mg/ml) was used as a templating agent to control the dispersion of the nanoparticles and nanoclusters formation. In this work, iron nitrate and PVP were mixed in 50 ml of ethylene glycol and stirred continuously until complete dissolution. 3 M of sodium acetate was added drop by drop and stirred for 45 min to form homogenous precipitates, which were transferred to a 100 ml Teflon-based autoclave for the solvothermal reaction at 180 °C for 8 hours. The obtained black solution was washed with ethanol and deionized water and dried at 80 °C for 6 hours to achieve Fe_3O_4 nanoparticles. The prepared samples will be referred to as Fe_3O_4_5, Fe_3O_4_10, and Fe_3O_4_25 for 5 mg/ml, 10 mg/ml, and 25 mg/ml of PVP, respectively.

The crystallinity and purity of the prepared sample were analyzed by the x-ray diffraction technique with Cu-K radiation (λ = 1.54 Å, X'pert Pro, PANalytical). Fourier transforms infrared (FTIR) spectroscopy was performed at room temperature using Perkin Elmer, spectrum 100 spectrometers with a wavenumber range from 400 cm^{-1} to 4000 cm^{-1} to analyze the interaction of the PVP molecule with the surface of the iron oxide nanoparticles. Field-emission transmission electron microscope (FE-TEM, FEI) equipped with the Energy-dispersive X-ray (EDS) spectrometer was used to analyze the morphology and dispersion of the nanoparticles. The magnetic hysteresis loop at room temperature was measured by the Lakeshore 7410 vibrating sample magnetometer.

3. Results and Discussion

Fig. 1(a) displays the XRD patterns of Fe_3O_4_5, Fe_3O_4_10, and Fe_3O_4_25 nanoparticles. The obtained diffraction peaks of all samples concern the cubic spinel structure of Fe_3O_4 according to the JCPDS n° 96-210-1927, without the presence of any impurities or secondary phases. The peaks were found to be broadened which indicates the nanometer-scale crystallinity of Fe_3O_4 particles [22]. To confirm the observed nano-crystallinity, we first calculated the crystallite size using the Debye-Scherrer formula and

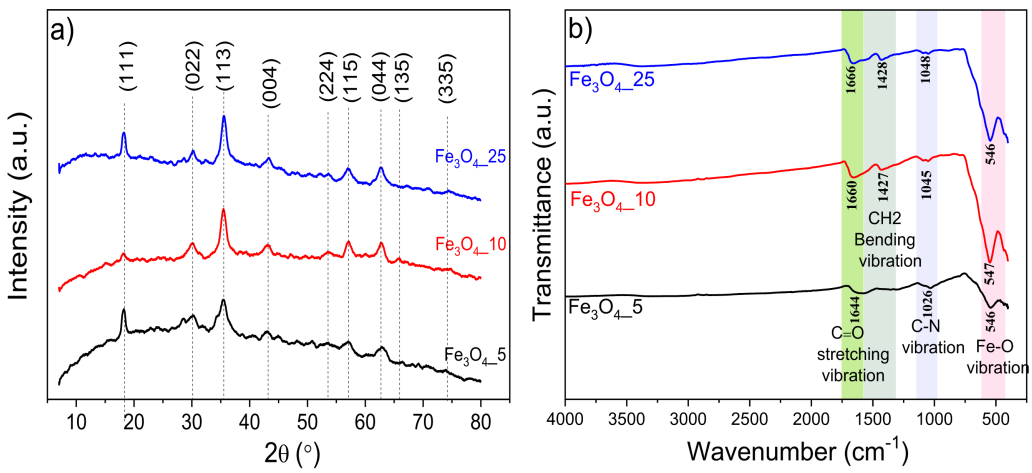

Fig. 1. (Color online) (a) XRD patterns, and (b) FT-IR spectrum at room temperature of the synthesized Fe_3O_4_5, Fe_3O_4_10, and Fe_3O_4_25 nanoparticles.

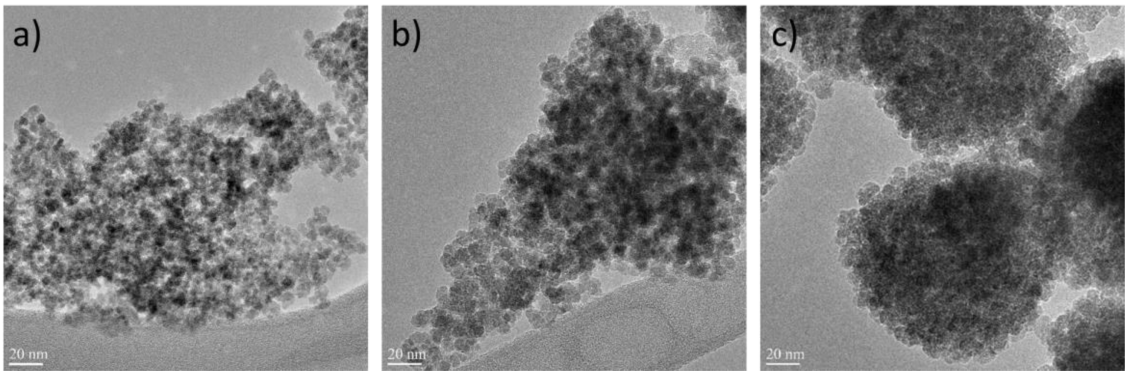

Fig. 2. TEM images of (a) Fe_3O_4_5, (b) Fe_3O_4_10, and (c) Fe_3O_4_25 nanoparticles.

it was found that the average crystallite size is smaller than 10nm for all Fe_3O_4 nanoparticles and increases with the increase of the concentration of PVP as listed in Table 1.

To analyze the presence of the PVP matrix in the prepared samples and its interaction with the surface of the nanoparticles, FTIR spectroscopy was performed at room temperature and presented in Fig. 1(b). As we can observe, a clear peak around 546 cm^{-1} is ascribed to the Fe-O bond absorption in all samples [22]. Moreover, the characteristic peaks of C=O (stretching vibration), CH_2 (bending vibration), and C-N (vibration) functional groups of the PVP molecule [21] were found around 1660 cm^{-1}, 1427 cm^{-1}, and 1045 cm^{-1}, respectively for Fe_3O_4_10 and around 1666 cm^{-1}, 1428 cm^{-1}, and 1048 cm^{-1}, respectively for Fe_3O_4_25.

TEM images of Fe_3O_4_5, Fe_3O_4_10, and Fe_3O_4_25 nanoparticles are presented in Fig. 2(a-c), respectively, at the same magnification. Small particle size was observed for all prepared samples. However, a clear difference in the dispersion of the nanoparticles is found depending on the concentration of the PVP matrix, where for a concentration up to 10 mg/ml, the nanoparticles show a homogeneous distribution. The aggregation of the

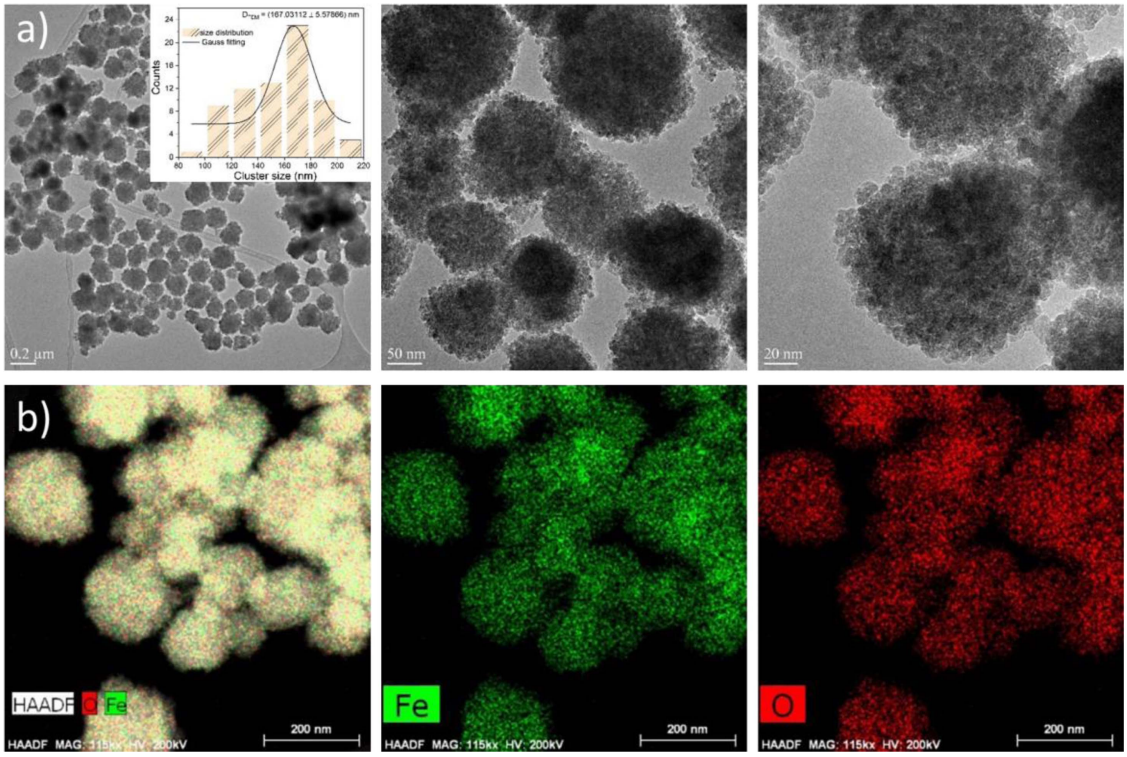

Fig. 3. (Color online) (a) TEM images of Fe_3O_4_25 nanoclusters with different magnifications, (b) EDS elemental mapping of Fe_3O_4_25 nanoclusters.

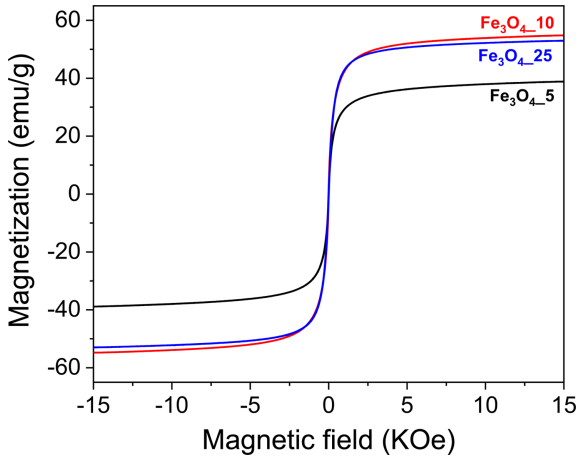

Fig. 4. (Color online) Magnetic hysteresis loop at room temperature of the prepared Fe_3O_4 nanoparticles.

nanoparticles is observed clearly for Fe_3O_4_25 as shown in Fig. 2(c). This aggregation can be explained by the interaction between the magnetic nanoparticles and the PVP which becomes stronger for high concentrations of the PVP leading to the formation of nanoclusters.

To further analyze the formation of Fe_3O_4 nanoclusters for a concentration of 25 mg/ml, Fig. 3(a-b) presents the TEM images and EDS mapping of Fe_3O_4_25 nanoparticles. As shown in Fig. 3(a), for a concentration of 25 mg/ml of PVP, the nanoparticles formed nanoclusters with almost spherical shape and homogenous size distribution with an average nanoclusters diameter of about 167 nm. The high magnifications of the TEM images showed that the nanoclusters consist of innumerable small iron oxide nanoparticles. Fig. 3(b) shows the energy-dispersive spectrum (EDS) elemental mapping of Fe_3O_4_25, where it is confirmed the presence of Fe and O elements in a uniform distribution in the nanoclusters.

Fig. 4 presents the magnetic hysteresis loop at room temperature of Fe_3O_4_5, Fe_3O_4_10, and Fe_3O_4_25 nanoparticles with magnetic parameters listed in Table 1. All prepared samples exhibit a ferromagnetic behavior where the coercivity was found to be 7.89 Oe, 9.20 Oe, and 9.78 Oe for Fe_3O_4_5, Fe_3O_4_10, and Fe_3O_4_25 nanoparticles, respectively. Generally, the magnetic properties of the nanoclusters can be different than the nanoparticle depending on the clustering method which affects the nanocluster size and inter-cluster interactions [23]. The saturation magnetization of the prepared samples increased from 38.81 emu/g for Fe_3O_4_5 to 54.75 emu/g for Fe_3O_4_10. Then, it decreases to 52.89 emu/g for Fe_3O_4_25. This slight decrease in the saturation magnetization in the nanoclusters (Fe_3O_4_25) compared to nanoparticles (Fe_3O_4_10) can be explained by the relatively high concentration of the Polyvinylpyrrolidone (PVP) binding to the surface of the aggregated nanoparticles which reduces the ferromagnetic interaction between the nanoparticles. The obtained magnetic properties of the nanoclusters can be further optimized by controlling the clustering of the nanoparticles through the modification of the concentration of the PVP in addition to the solvothermal synthesis parameters.

Table 1. Crystallite size (nm), saturation magnetization (emu/g), and coercivity (Oe) of Fe_3O_4_5, Fe_3O_4_10, and Fe_3O_4_25 nanoparticles

	Crystallite size (nm)	Saturation magnetization (emu/g)	Coercivity (Oe)
Fe_3O_4_5	3.39	38.81	7.89
Fe_3O_4_10	6.27	54.75	9.20
Fe_3O_4_25	6.34	52.89	9.78

4. Conclusion

This work presented the synthesis of Fe_3O_4 nanoparticles using a one-pot solvothermal method, and the effects of PVP on the structural, microstructural, and magnetic properties. The microstructural analysis indicated a dependence of the dispersion of the nanoparticles to the concentration of the PVP where high concentration leads to the formation of nanoclusters with homogeneous size distribution around 167 nm. Fe_3O_4 nanoparticles with 10 mg/ml of PVP exhibit the highest saturation magnetization of 54.75 emu/g compared to 38.81 emu/g, and 52.89 emu/g, for 5 mg/ml, and 25 mg/ml, respectively.

Acknowledgment

This work was supported by the 2022 Yeungnam University Research Grant.

References

[1] L. S. Ganapathe, M. A. Mohamed, R. M. Yunus, and D. D. Berhanuddin, Magnetochemistry **6**, 68 (2020).
[2] X. Yu, C. F. Huo, Y. W. Li, J. Wang, and H. Jiao, Surf. Sci. **606**, 872 (2012).
[3] H. Ardiyanti, E. Suharyadi, T. Kato, and S. Iwata, AIP Conf. Proc. **1725**, (2016).
[4] A. K. Sidhu, N. Verma, and P. Kaushal, Front. Nanotechnol. **3**, 105 (2022).
[5] R. Javed, M. Zia, S. Naz, S. O. Aisida, N. ul Ain, and Q. Ao, J. Nanobiotechnology **18**, 1 (2020).
[6] Y. Zare, Compos. Part A Appl. Sci. Manuf. **84**, 158 (2016).

[7] W. Wang, B. Tang, B. Ju, and S. Zhang, RSC Adv. **5**, 92 (75292).
[8] Z. Lu and Y. Yin, Chem. Soc. Rev. **41**, 6874 (2012).
[9] P. Bender *et al*., Nanotechnology **29**, 425705 (2018).
[10] J. D. Aiken and R. G. Finke, J. Mol. Catal. A Chem. **145**, 1 (1999).
[11] Z. Lu and Y. Yin, Chem. Soc. Rev. **41**, 6874 (2012).
[12] J. Ge, Y. Hu, M. Biasini, W. P. Beyermann, and Y. Yin, Angew. Chemie - Int. Ed. **46**, 4342 (2007).
[13] A. J. Antone, Z. Sun, and Y. Bao, Magnetochemistry **5**, 45 (2019).
[14] S. Pandit and S. Kundu, Lumin. Met. Nanoclusters Synth. Charact. Appl. 17 (2022).
[15] Z. Xiao, L. Zhang, V. L. Colvin, Q. Zhang, and G. Bao, Ind. Eng. Chem. Res. **61**, 7613 (2022).
[16] J. Ge, Y. Hu, M. Biasini, W. P. Beyermann, and Y. Yin, Angew. Chemie Int. Ed. **46**, 4342 (2007).
[17] W. Wang *et al.*, J. Magn. Magn. Mater. **423**, 111 (2017).
[18] J. Gao, X. Ran, C. Shi, H. Cheng, T. Cheng, and Y. Su, Nanoscale **5**, 7026 (2013).
[19] S. Xuan, Y. X. J. Wang, J. C. Yu, and K. C. F. Leung, Chem. Mater. **21**, 5079 (2009).
[20] F. Y. Alzoubi *et al.*, J. Compos. Sci. **7**, 131 (2023).
[21] K. M. Koczkur, S. Mourdikoudis, L. Polavarapu, and S. E. Skrabalak, Dalt. Trans. **44**, 17883 (2015).
[22] J. Siregar, K. Sebayang, B. Yuliarto, and S. Humaidi, AIP Conf. Proc. **2221**, (2020).
[23] Z. Xiao, L. Zhang, V. L. Colvin, Q. Zhang, and G. Bao, Ind. Eng. Chem. Res. **61**, 7613 (2022).